Protein Extractions with Hollow Fibers

Differential protein extractions were measured with two types of extractants: inverted micelles and two-phase aqueous systems. The results show that hollow-fiber extractions are substantially faster than those possible in conventional equipment. The extractions are not compromised by loading or flooding because the flows of extractant and raffinate are almost completely independent. Mass transfer coefficients inferred from the measurements both support and extend design equations for these contactors.

Lise Dahuron, E. L. Cussler
Chemical Engineering and
Materials Science
University of Minnesota
Minneapolis, MN 55455

Introduction

This paper uses microporous hollow-fiber contactors to achieve two goals. First, it shows how these contactors can be used to extract proteins such as those produced by genetic engineering. Second, it extends correlations used for designing these contactors.

The rationale for these goals is founded both on the potential advantages of hollow fibers and on the basic chemistry of proteins. The advantages of hollow fibers center on their large surface area per volume a. In particular, these systems routinely have surface areas of 30 cm^2/cm^3 (1,000 ft^2/ft^3), and values ten times larger have been claimed (Matson et al., 1983). While the mass transfer coefficient K is not unusually high in fibers, the product Ka is often 10 to 50 times larger than in conventional extraction towers (Zhang and Cussler, 1985a; Kiani et al., 1984). Moreover, in hollow fibers the two fluid flows are almost completely independent. As a result there is no constraint due to flooding, to loading, or to channeling (Kim, 1984; Cooney and Jim, 1984; D'Ella et al., 1986). Hollow fibers appear to be a superior way to achieve fast mass transfer.

The second half of the rationale, that of protein chemistry, begins with the production of proteins by genetically engineered microorganisms or mammalian cells. These proteins are often produced in a highly dilute solution that must be dramatically concentrated and purified (Belter et al., 1988). Liquid extraction is one attractive route for this purification. However, the extraction solvents used for proteins are unconventional. One type is an alkane solution of oil-soluble detergent (Göklen and Hatton, 1987). Proteins are solubilized within inverted detergent micelles, and hence protected from denaturation by the surrounding hydrophobic environment. The second type is two immiscible aqueous phases (Kula et al., 1982). One of these contains mixed potassium phosphates, and the other contains polyethylene glycols. Both the inverted micelle extractions and the two-phase aqueous extractions are known to offer substantial selectivity, and hence are valuable process developments for bioseparations.

The protein extraction studies also yield another, more basic dividend. The studies produce overall mass transfer coefficients that can be compared with those expected from hollow-fiber design equations developed from gas absorptions and from heat transfer (Yang and Cussler, 1986; Prasad and Sirkar, 1987). This comparison can be difficult, for the overall coefficients represent a sum over mass transfer in the extractant, in the raffinate, and across the membrane. When these difficulties can be overcome, we can make very demanding comparisons, because the Schmidt numbers involved vary by more than 30,000.

In the next section we describe the construction and operation of the hollow-fiber modules, including the calculation of the mass transfer coefficient. We then discuss the results, including both the successes and the shortcomings of this type of experiment. Finally, we compare the mass transfer coefficients found for proteins with those expected from correlations based on gas absorption and heat transfer.

Experimental Method

Materials

All materials were used as received. The reagent grade organic solvents are isobutanol (Aldrich), isooctane (2,2,4-trimethylpentane) (Aldrich), and 2-heptanone (Alfa Products). The acetic acid solution is made by diluting glacial acetic acid (Hipure Chemicals) with freshly distilled water. All salts are reagent grade: dibasic potassium phosphate (Mallinckrodt), monobasic potassium phosphate (Spectram) and potassium chloride (Spectram). The polyethylene glycol (P-3640, Sigma) has a molecular weight of 3,350. Aerosol OT (AOT) of the purest commercial form is made by Pfaltz and Bauer. Other solutes are from Sigma: spectrophotometric grade p-nitrophenol, type III myoglobin from horse heart, type II α-chymotrypsin from

bovine pancreas, type III cytochrome-c from horse heart, catalase from bovine liver, and type II urease from jack beans.

Apparatus

The membrane modules used in this work, which look like small shell-and-tube heat exchangers, are made with Celgard 2500 microporous polypropylene hollow fibers (Questar, Charlotte, NC). Sixty fibers 15 to 20 cm long are mounted in glass tubes of 0.8 cm ID and 0.2 cm wall thickness. The fibers are glued in place with epoxy (FE 5045, H. B. Fuller, St. Paul, MN). This epoxy is unaffected by a wide variety of organic solvents (D'Elia, 1985) and is rigid enough to be cut without crushing the ends of the fibers. The epoxy is also poured into a Teflon mold at the end of the module; when this mold is removed, it leaves a threaded connection. Further details of this construction are given elsewhere (Dahuron, 1987).

The completed module is installed in the apparatus shown in Figure 1. In this apparatus, a feed solution circulates from a feed reservoir of 100 cm^3 volume, through a positive displacement pump (FMI model RP-D2), through the module, and back into the feed reservoir. The extractant circulates either cocurrently or countercurrently from a 100 cm^3 reservoir, through a similar pump, through the module, and back into the extractant reservoir. The solute concentrations in the two reservoirs are measured as a function of time; these measurements alter the volumes in the reservoir by less than 1%.

The key to the apparatus is the adjustment of the four valves shown in Figure 1. Obviously, these four valves can be used to adjust the flow rates of feed and extractant; less obviously, they can be used to adjust the static pressure across the microporous membranes. This adjustment of static pressure is important. The membranes in the module are preferentially wetted by one phase. This phase fills the membrane pores, and wicks through the pores to the other side of the membrane. As a result, the interface between the wetting and nonwetting liquids tends to move to the nonwetting surface of the membranes. There, it can shear off to form an emulsion (D'Elia et al., 1986).

This emulsion formation can be eliminated by using the four valves to apply a higher static pressure to the nonwetting fluid (Kiani et al., 1984). Such a static pressure pushes the liquid-liquid interface back into the membrane pores. There the interface is unaffected by shear and emulsions do not form. Such an adjustment of static pressure is especially important for liquids such as those used here, which show similar densities and almost equal interfacial tensions.

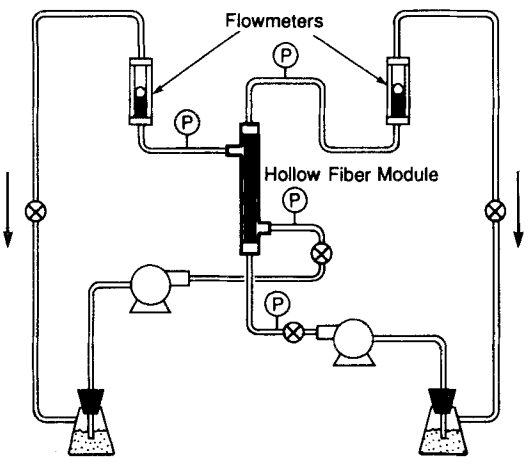

Figure 1. Apparatus.
Fluid pressure across fiber membranes can be adjusted to stabilize liquid-liquid interface within membrane pores

The measurement of solute concentration depends on the particular solute under study (Snell and Hitton, 1966). Acetic acid concentrations are measured by titration with sodium hydroxide, using phenolphthalein as an indicator. *p*-nitrophenol concentrations were measured by spectrophotometry at 310 nm, using a Beckman model DU50 UV-visible instrument. Protein concentrations were measured at 280 nm with the same device. These measurements were used to find both equilibrium partition coefficients and mass transfer coefficients.

The overall mass transfer coefficients can be calculated from these concentration measurements. In general, the algebraic form of this calculation is complicated (Zhang and Cussler, 1985b; Dahuron, 1987). For cocurrent flow, the result is

$$\ln\frac{\Delta c}{\Delta c_o} = -t\left\{\left(\frac{\frac{1}{V_{in}}+\frac{1}{HV_{out}}}{\frac{1}{Q_{in}}+\frac{1}{HQ_{out}}}\right)\left[1-e^{-4K_{in}\ell/dv_{in}(1+Q_{in}/HQ_{out})}\right]\right\} \quad (1)$$

The symbols are defined in the Notation. For countercurrent flow, the result is

$$\ln\frac{\Delta c}{\Delta c_o} = -t\left\{\left[Q_{in}\left(\frac{1}{V_{in}}+\frac{1}{HV_{out}}\right)\right]\cdot\left[\frac{1-e^{-4K_{in}\ell/dv_{in}(1-Q_{in}/HQ_{out})}}{1-\frac{Q_{in}}{HQ_{out}}e^{-4K_{in}\ell/dv_{in}(1-Q_{in}/HQ_{out})}}\right]\right\} \quad (2)$$

For both cocurrent flow and countercurrent flow, the concentration differences on the lefthand sides of Eqs. 1 and 2 are given by

$$\ln\frac{\Delta c}{\Delta c_o} = \ln\left[\frac{c_{in}\left(1+\frac{V_{in}}{HV_{out}}\right)-\frac{c^o_{in}V_{in}}{HV_{out}}-\frac{c^o_{out}}{H}}{c^o_{in}-\frac{c^o_{out}}{H}}\right] \quad (3)$$

We use all three equations in the analysis that follows.

Results

In this section we report the overall mass transfer coefficients for protein extractions. The results include seven proteins in two different extraction systems and under a wide variety of flows. Data for the small solutes *p*-nitrophenol and acetic acid are also included. The section is a summary of extensive data tabulated elsewhere (Dahuron, 1987), and has three parts. First, we show that the extraction data do in fact fit Eqs. 1–3, and hence permit calculation of the mass transfer coefficients. Second, we present typical values of these coefficients, and show how they vary with feed and extractant flows. Third, we describe the characteristics and the difficulties of these experiments. We defer a discussion of correlations of the coefficients until the next section.

That the data do fit Eq. 1 is exemplified by the results in Fig-

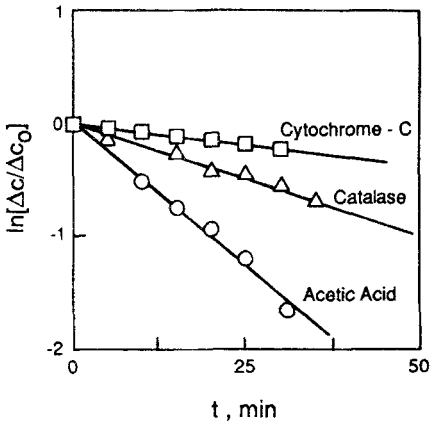

Figure 2. Solute concentration vs. time.

Solute concentration plotted on the ordinate is the function given in Eq. 3; the slope of this function vs. time is related to the mass transfer coefficient by Eqs. 1 and 2.

ure 2. In this figure the ordinate is the concentration difference given by Eq. 3, and the abscissa is the time. As expected, the variation is linear for the acetic acid, for cytochrome-c in the inverted micelles, and for catalase in the two-phase aqueous extraction. The reproducibility of the data in all cases is good. The slopes in Figure 2 are measures of the mass transfer coefficient.

We can calculate the mass transfer coefficient K_{in} from these slopes by means of the terms in braces in Eqs. 1 and 2. These slopes are complicated functions of known parameters. They are functions of module properties such as the fiber diameter d, of apparatus properties such as the reservoir volume V_{out}, and of operating parameters such as the total flow within the fibers Q_{in}. The only unknown parameter in these equations is K_{in}.

We can calculate the mass transfer coefficient K_{in} from data like those in Figure 2 because we know the surface area per volume $a(= 4/d)$. Knowing this quantity, a direct consequence of our use of hollow fibers, is unusual. In most mass transfer experiments we can measure only the product $K_{in}a$ or its equivalent. As a result, we do not know how much of the observed rate is due to diffusion, included in K_{in}, and how much is due to area, contained in a. The experiments in this paper do not have this uncertainty.

Examples of mass transfer coefficients found from plots like Figure 2 are given in Table 1. The first column in this table gives the solute being transferred; the second, third, and fourth columns give the solvent inside the fibers, that within the membrane pores, and that outside the fibers. The next three columns give the partition coefficient, defined as the equilibrium concentration in the outside solvent divided by that in the inside solvent, and the velocities within and outside the fibers. The velocity outside is in fact the superficial velocity, the volumetric flow divided by the cross-sectional area of the tube.

The final column in Table 1 gives the mass transfer coefficient. The mass transfer coefficients for the small solutes range from 10^{-3} to 10^{-6} cm/s, which is the range commonly observed (Treybal, 1980; Cussler, 1984). In the simplest terms, these coefficients should equal the diffusion coefficient, which is around 10^{-5} cm^2/s, divided by the boundary layer thickness, around 10^{-2} cm. This gives a value close to the highest observed. Decreases can be caused either by the partition coefficient H or by the mass transfer resistance of the membrane itself. We defer untangling these causes until the next section.

The mass transfer coefficients for the seven proteins, which are also shown in Table 1, fall within the range of those observed for the small solutes, but average somewhat below them. This lower average is expected, because the diffusion coefficients of the macromolecular proteins are significantly less than those of small solutes such as p-nitrophenol. Again, we expect that the partition coefficient H and the membrane resistance are influential, and will explore this later.

The fact that the values of K_{in} for proteins do fall within the range of values for small solutes implies that no extraordinary mechanism exists for protein transport. In particular, the membrane may offer a resistance due to diffusion, but it apparently offers no resistance due to ultrafiltration. If an ultrafiltration

Table 1. Typical Values of Mass Transfer Coefficients for Protein and Other Extractions

Solute	Solvent Inside	Membrane Solvent	Solvent Outside	H	v_{in} cm/s	v_{out} cm/s	K_{in} cm/s
Acetic acid	Water	Heptanone	Heptanone	0.4	29.0	6.6	2.1×10^{-4}
p-Nitrophenol	Water	Amyl acetate	Amyl acetate	70	28.6	6.1	3.4×10^{-3}
	Water	Isobutanol	Isobutanol	29	18.8	4.8	9.0×10^{-4}
	Isobutanol	Isobutanol	Water	0.035	42.5	1.5	1.3×10^{-5}
	Heptanone	Heptanone	Water	0.0025	65.0	5.0	5.1×10^{-6}
	Water	Heptanone	Heptanone	400	21.8	3.8	2.8×10^{-3}
Cytochrome-c	Phosphate buffer	PEG	PEG	0.18	16.3	6.6	5.5×10^{-6}
Myoglobin	Phosphate buffer	PEG	PEG	0.009	4.0	5.0	7.5×10^{-7}
α-Chymotrypsin	Phosphate buffer	PEG	PEG	0.16	16.3	1.9	7.0×10^{-6}
Catalase	Phosphate buffer	PEG	PEG	0.12	16.3	5.0	2.8×10^{-5}
Urease	Phosphate buffer	PEG	PEG	0.65	16.3	5.0	2.0×10^{-4}
Cytochrome-c	Phosphate buffer	AOT in octane	AOT in octane	4	13.3	8.8	1.3×10^{-4}
α-Chymotrypsin	Phosphate buffer	AOT in octane	AOT in octane	10	20.0	8.8	1.7×10^{-4}

resistance did exist, it would presumably retard urease the most, because urease is the largest of the proteins (mol. wt. 250,000 dalton). Instead, urease has the highest value of K_{in} among the proteins.

The apparently normal values of the protein K_{in}'s also argue against any interfacial resistance. This is most easily imagined for the extraction and stripping of the protein cytochrome-c from water into an isooctane solution of Aerosol OT (Göklen and Hatton, 1987). Cytochrome-c, which has a molecular weight of 13,370, forms red solutions, so analysis is easy. Aerosol OT (AOT) solubilizes proteins below their isoelectric points with only minor denaturation. It is the pH and the ionic strength of the aqueous solution that determine the partition coefficient, and hence whether extraction or stripping occurs.

Mass transfer in this system begins when cytochrome-c diffuses through water to the water-octane interface, and reacts with AOT to produce a mixed micelle. The mixed micelle then diffuses through the membrane and into the bulk octane. If the reaction producing the mixed micelle were much slower than the diffusion steps, it would reduce the value of K_{in}. Such a reduction could alter the selectivity of the separation. However, because no such reduction occurs, there is no major effect of an interfacial resistance.

Finally, we want to detail experimental problems with individual protein extractions. First, we consider the inverted micelle extraction. We found two major problems with this system. The first is that some of the surfactant adsorbs on the hydrophobic surface of the membrane, reducing the surface tension between the membrane and both the oganic and the aqueous phases. As a result, the capillary pressure, which stabilizes the liquid-liquid interface inside the pores, is dramatically reduced. This means that we must carefully adjust the static pressure difference across the membrane to avoid emulsification.

Our second problem with inverted micelles was protein denaturation. Initially, running the system for a few minutes produced precipitated protein. The most probable cause of denaturation was shear in the pump, but running the system without the fiber module produced no denaturation. We next thought that the fibers themselves caused the denaturation. Later, however, we found that the key was insuring that no air was trapped in the apparatus. When trapped air was carefully removed, no denaturation occurred.

We found different problems with the two-phase aqueous experiments. We expected that the high viscosity of the polyethylene glycol systems might cause trouble, but we avoided this by keeping the polyethylene glycol on the shell side of the modules. We had much more difficulty with emulsion formation caused by the extremely low surface tension between the two solutions. Again we could stop emulsion formation simply by careful adjustment of the static pressures. We now turn from these details to more general characteristics of the results.

Discussion

The results above show that protein extractions with hollow-fiber modules offer faster separations than are possible in conventional equipment. This fast extraction is not the result of large mass transfer coefficients: the mass transfer coefficients shown in Table 1 have the values expected for large solutes such as proteins. Instead, the fast extraction is the result of the large surface area per volume in these modules (Zhang and Cussler, 1985a,b; Prasad et al., 1986). This speed can be achieved even when the feed and extractant have nearly equal densities. It can be achieved without the constraints of loading and flooding.

The results for protein extraction also permit development of better design equations for hollow-fiber contactors. These design equations have already been developed for gas absorption (Yang and Cussler, 1986), and now can be extended to liquid-liquid systems. This broader goal is the subject of this section.

To achieve this goal, we must return to the definition of the overall mass transfer coefficient used in presenting the results above. The reciprocal of this overall mass transfer coefficient is the total resistance to mass transfer in these modules (Treybal, 1980; Cussler, 1984). This resistance is in turn the sum of the mass transfer resistances inside the fiber, across the fiber wall, and in the solution surrounding the fibers:

$$\frac{1}{K_{in}} = \frac{1}{k_{in}} + \frac{1}{k_{mem}} + \frac{1}{k_{out}H} \tag{4}$$

where k_{in}, k_{mem}, and k_{out} are the individual mass transfer coefficients inside the fiber, across the fiber wall, and outside the fibers, and H is again the partition coefficient: the concentration at equilibrium in the outer solution divided by that in the inner solution. This result differs from that in a convectional mass transfer device only in the appearance of the membrane resistance $1/k_{mem}$ (Zhang and Cussler, 1985a,b).

Membrane resistance

Each of the coefficients on the righthand side of Eq. 2 has characteristics that merit separate discussion. The coefficient k_{mem} is the simplest, for it refers only to diffusion across the membrane. If the membrane is wet by the inner solution, then

$$k_{mem} = \frac{D}{\delta} \tag{5}$$

where D is the diffusion coefficient in the membrane, and δ is the effective membrane thickness. This effective thickness, which includes both the void fraction and the pore tortuosity of the particular membrane, cannot often be estimated theoretically, but must be found by experiment. If the membrane is wet by the outer solution, the result is

$$k_{mem} = \frac{DH}{\delta} \tag{6}$$

While this is mathematically similar to Eq. 5, it can be dramatically different numerically, for H is often significantly different than one.

Equations 5 and 6 show that k_{mem} does depend on the diffusion coefficient of the solute in the solvent within the pores. It depends on the membrane properties, lumped into the single effective thickness δ. It does not depend on the conditions in the adjacent solutions, including their flows. These conditions affect only k_{in} and k_{out}.

Extractions controlled inside fibers

The values of k_{in} and k_{out} are most conveniently organized as dimensionless correlations. For fiber modules, the appropriate correlations give the Sherwood number as a function of the Rey-

nolds number, the Schmidt number, and the ratio of a diameter per fiber length (Yang and Cussler, 1986):

$$\left(\frac{kd}{D}\right) = (A)\left(\frac{dv}{\nu}\right)^{\alpha}\left(\frac{\nu}{D}\right)^{\beta}\left(\frac{d}{\ell}\right)^{\gamma} \tag{7}$$

where A, α, and β and γ are adjustable parameters. Of course, there are four of these parameters for k_{in} and four more for k_{out}, giving a total of eight. Such a plethora of parameters is more than the accuracy of our data can possibly justify.

As a result, we have tried to separate the effects of k_{in} and k_{out} by plotting the reciprocal of k_{in} vs. the reciprocal of some power of the velocity, a method sometimes referred to as a Weber plot. For k_{in} this usually involves making experiments at large constant v_{out}, so that k_{out} is minimized. From previous theories, from experiments with fibers for gas absorption, and from heat transfer analogies, we expect that $\alpha = \beta = \gamma = 1/3$. Equations 4 and 7 can then be combined to give

$$\frac{1}{K_{in}} = \left(\frac{1}{k_{mem}} + \frac{1}{k_{out}H}\right) + \frac{d}{AD}\left(\frac{\ell D}{d^2 v_{in}}\right)^{1/3} \tag{8}$$

Thus a plot of K_{in}^{-1} vs. $v_{in}^{-1/3}$ gives a slope from which the constant A can be determined. The intercept on this plot represents the total membrane and outside resistance for each chemical system studied.

To determine A, we need to estimate the diffusion coefficient D in the unusual solutions used to these extractions. For small electrolytes, we use experimental values in water, and we estimate values in organic solvents using these aqueous values and the Wilke-Chang correlation (Cussler, 1984). For proteins in the two-phase aqueous extractions, we use experimental values in water (Cantor and Schimmel, 1980; Zubay, 1983). For proteins in inverted micelles, we know no way to make estimates and so omit these data from our correlations. We find that

$$\frac{k_{in}d}{D} = 1.5\left(\frac{d^2 v}{\ell D}\right)^{1/3} \tag{9}$$

close to the results reported over the last sixty years. Data are compared with predictions of this result in Figure 3, showing the agreement obtained.

Extractions controlled outside fibers

We used a similar strategy to find k_{out}. First, we consider cases with a large fixed value for v_{in}. From previous experiments with hollow fibers, we expect that $\alpha = \gamma = 1$. Equations 4 and 7 can now be combined to give

$$\frac{1}{K_{in}} = \left(\frac{1}{k_{in}} + \frac{1}{k_{mem}}\right) + \frac{d_e}{ADH}\left(\frac{\ell\nu}{d_e^2 v}\right)\left(\frac{D}{\nu}\right)^{\beta} \tag{10}$$

where the constants A and β must be found empirically. The diffusion coefficients D are estimated as before. The result is

$$\frac{k_{out}d_e}{D} = 8.8\left(\frac{d_e^2 v}{\ell\nu}\right)\left(\frac{\nu}{D}\right)^{1/3} \tag{11}$$

The agreement between calculated and observed results in this case is shown in Figure 4.

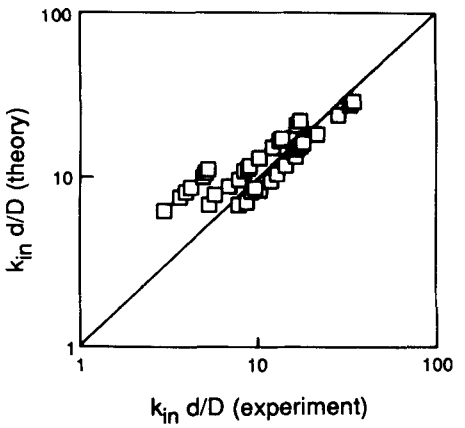

Figure 3. Mass transfer coefficients inside hollow fibers.
Coefficients shown, based on cases where k_{in} dominates K_{in}, provide a test of Eq. 9

Comparing correlations

The correlations in Eqs. 9 and 11 are close to many correlations suggested earlier, as shown in Table 2. For flow inside the fibers, the mass transfer coefficient varies with the cube root of the liquid velocity, as suggested by earlier correlations. It varies with the 2/3 power of the diffusion coefficient, consistent with earlier fiber experiments (Yang and Cussler, 1986), with heat transfer studies (Sieder and Tate, 1936), and with theory (Lévêque, 1928). The diffusion coefficients used in this study range over three orders of magnitude, more than in earlier studies. The constant of 1.5 found here is close to the range of 1.6 to 1.9 found earlier.

The correlation for flow outside the fibers seems consistent with our earlier fiber studies (Yang and Cussler, 1986). The mass transfer coefficient varies linearly with Reynolds number, which is not dramatically different from the change found in other fiber experiments (Yang and Cussler, 1986). Our data are not consistent with the 0.6 power of flow (Prasad and Sirkar, 1987). This difference is possibly due to different channeling around the fibers. The mass transfer coefficient varies with diffusion coefficient to the 2/3 power, a point not checked in earlier fiber experiments. All hollow-fiber correlations are different from earlier heat transfer results, although these are for some-

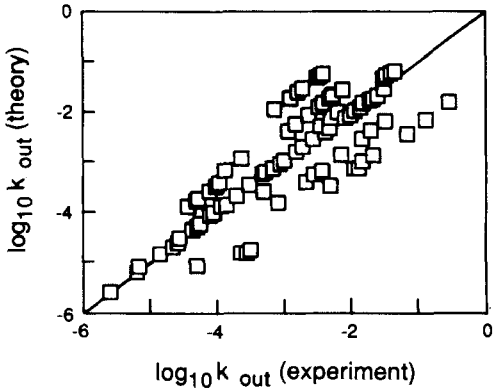

Figure 4. Individual mass transfer coefficients outside hollow fibers.
These coefficients stress cases where k_{out} dominates K_{in}, and hence test Eq. 11

Table 2. Mass Transfer Correlations

Conditions	This Work	Other Fiber Results	Nonfiber Results	Remarks
Laminar flow inside fibers	$\frac{kd}{D} = 1.5\left(\frac{d^2v}{\ell D}\right)^{1/3}$	$\frac{kd}{D} = 1.64\left(\frac{d^2v}{\ell D}\right)^{1/3}$*	$\frac{kd}{D} = 1.61\left(\frac{d^2v}{\ell D}\right)^{1/3}$***	In these cases, d is the internal fiber diameter.
			$\frac{kd}{D} = 1.86\left(\frac{d^2v}{\ell D}\right)^{1/3}$†	
Laminar flow outside fibers	$\frac{kd_e}{D} = 8\left(\frac{d^2v}{\ell\nu}\right)\left(\frac{\nu}{D}\right)^{1/3}$	$\frac{kd_e}{D} = 5.9\left(\frac{d_e}{\ell}\right)\left(\frac{d_e v}{\nu}\right)^{0.6}\left(\frac{\nu}{D}\right)^{1/3}$**	$\frac{kd_e}{D} = 0.22\left(\frac{d_e v}{\nu}\right)^{0.8}\left(\frac{\nu}{D}\right)^{1/3}$†	The characteristic length d_e is defined as four times the cross section divided by the wetted perimeter
		$\frac{kd_e}{D} = 1.25\left(\frac{d_e^2 v}{\ell\nu}\right)^{0.93}\left(\frac{\nu}{D}\right)^{1/3}$*	$\frac{kd_e}{D} = 0.23\left(\frac{d_e v}{\nu}\right)^{0.60}\left(\frac{\nu}{D}\right)^{1/3}$‡	

*Yang and Cussler (1986); results for gas absorption, not liquid extraction
**Prasad and Sirkar, 1987
***Leveque (1928); a theoretical result
†Sleder and Tate (1936). Heat transfer results. The first is for liminar flow; the second is for turbulent flow within fibers, included here because it seems in closer agreement with the observations.
‡Krieth and Black (1980); a heat transfer result

what different physical conditions. The numerical constant of 8.8 found here is significantly larger than that of 1.3 found in the earlier fiber studies.

Overall, the correlations found for hollow fibers give a Sherwood number that varies as expected with Graetz, Reynolds, and Schmidt numbers. This success depends on the accuracy of the diffusion coefficients, especially of the proteins. We often have no direct measures of these coefficients. When we use the solution viscosity to estimate them from the existing correlations (Cussler 1984), we predict mass transfer coefficients that scatter widely. When we use instead the diffusion coefficients in water, we get much more consistent values. Previous workers who were studying conductance and diffusion in polymer solutions have also obtained more consistent results using the solvent viscosity (Komiyana and Fuoss, 1972; Hiss and Cussler, 1973). They argued that long-range entanglements influenced viscosity but not diffusion. They distinguished between a macroscopic viscosity measured in the viscometer, and a microscopic viscosity felt by the solutes as they diffuse. Such a rationalization can also be used to support the results obtained here. This rationalization seems reasonable but is without direct experimental support.

Intermediate cases

The correlations found above, based on cases where one mass transfer resistance is isolated, allow us to consider more complicated cases where no single mass transfer resistance is dominant. To do so, we need to fix only one additional parameter, the effective thickness of the membrane. From a wide variety of experiments, we found that δ equals 0.04 cm for small electrolytes and 0.015 cm for proteins. This implies a tortuosity of 3 in

Table 3. Calculated vs. Experimental Values Overall Mass Transfer Coefficient for Proteins

Solute	$\frac{1}{k_{in}}$	$\frac{\delta}{D}$	$\frac{1}{k_{mem}}$	$\frac{1}{k_{out}}$	$\frac{1}{k_{out}H}$	K_{in} theory cm/s	K_{in} exp cm/s
Acetic acid from water into heptanone	500 (10%)	1,800	4,500 (85%)	100	250 (5%)	2.2×10^{-6}	2.1×10^{-6}
p-Nitrophenol from water into amyl acetate	400 (93%)	1,600	20 (5%)	300	7 (2%)	2.3×10^{-3}	2.7×10^{-3}
p-Nitrophenol from water into *i*-butanol	600 (52%)	12,000	600 (41%)	2,000	70 (7%)	9.9×10^{-4}	9.3×10^{-4}
p-Nitrophenol from *i*-butanol into water	800 (3%)	13,000	13,000 (47%)	500	14,000 (50%)	3.6×10^{-5}	2.2×10^{-5}
p-Nitrophenol from heptanone into water	200 (0%)	150,000	150,000 (65%)	200	80,000 (35%)	4.3×10^{-6}	5.1×10^{-6}
p-Nitrophenol from water into heptanone	2,000 (2%)	13,000	72,000 (91%)	1,000	5,500 (7%)	1.3×10^{-5}	1.3×10^{-5}
Cytochrome-c from buffer into PEG	2,000 (0%)	13,000	1.5×10^6 (93%)	1,000	110,000 (7%)	6.2×10^{-7}	6.5×10^{-7}
Myoglobin from buffer into PEG	3,000 (3%)	15,000	78,000 (91%)	1,000	5,500 (6%)	1.1×10^{-5}	1.3×10^{-5}
α-Chymotrypsin from buffer into PEG	4,000 (8%)	5,000	30,000 (59%)	3,000	17,000 (33%)	3×10^{-6}	1.5×10^{-6}
Catalase from buffer into PEG	5,000 (55%)	small	small (0%)	5,500	6,000 (45%)	1.2×10^{-5}	8×10^{-6}
Urease from buffer into PEG	2,000 (17%)	8,000	2,000 (17%)	30,000	7,500 (66%)	1.2×10^{-4}	1.3×10^{-4}

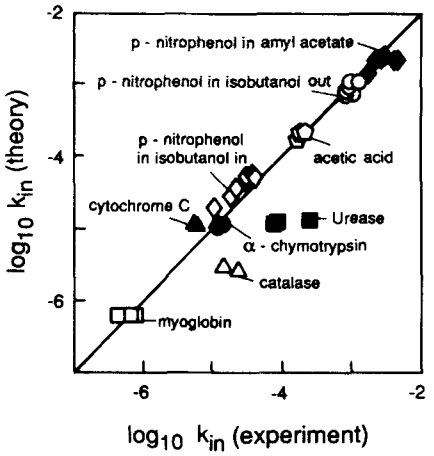

Figure 5. Overall mass transfer coefficients.
Success of the correlations in Table 2 is illustrated by agreement between estimated and experimental values of K_{in}

these membranes, which is somewhat higher than those found by others for similar microporous polypropylene membranes (Kiani et al., 1984; Prasad and Sirkar, 1987).

With this tortuosity, we can now calculate the mass transfer coefficients and the resistances for a wide variety of liquid-liquid extractions, as shown in Table 3. The first column in this table describes the physical systems, which are the same as those in Table 1, but at slightly different flow rates (Dahuron, 1987). The second column, calculated from Eq. 8, gives the resistance inside the fiber, and in parentheses the fraction which that resistance is of the total. The third and fourth columns use Eqs. 5–6 to do the same for the membrane. The fifth and sixth columns use Eq. 11 to find the mass transfer coefficient and the resistance outside the fibers. The final two columns compare the estimated and experimental values of the overall mass transfer coefficient K_{in}.

The results in Table 3 show that liquid-liquid extraction in hollow-fiber modules is complex. No single resistance dominates all the time. For example, for myoglobin, the resistance inside the fibers is not important; for urease, the resistance outside the fibers is not important; for *p*-nitrophenol, the resistance across the membrane is not important. One resistance is dominant only in a few special cases.

Even though these extractions are complex, their rate can be estimated using the correlations in Table 3. The success of these correlations is shown in Figure 5. Some systems deviate from the predictions, and show mass transfer coefficients different than expected. More agree closely with the predictions. These successes and the correlations that they imply represent the real accomplishment of this work.

Acknowledgment

The authors benefitted from conversations with Kent Göklen of Merck and T. Alan Hatton of the Massachusetts Institute of Technology. The research was principally supported by the Celanese Corporation; other significant support came from the National Science Foundation, Grant Nos. 84-08999 and 86-11646.

Notations

a = interfacial area per volume
A = constant
c = solute concentration
c^o = initial solute concentration
d = fiber diameter
d_e = equivalent diameter, 4 (wetted perimeter/cross section)
D = diffusion coefficient
H = partition coefficient
k = individual mass transfer coefficient, Eq. 4
K_{in} = overall mass transfer coefficient
ℓ = fiber length
Q_{in}, Q_{out} = volumetric flows of inner and outer fluids
v = velocity
V_{in}, V_{out} = reservoir volumes of inner and outer fluids

Greek letters

α, β, γ = exponents
δ = effective membrane thickness
ν = kinematic viscosity

Literature Cited

Belter, P. A., E. L. Cussler, and Wei-Shou Hu, *Bioseparations*, Wiley, New York (1987).
Cantor, C. R., and P. R. Schimmel, *Biophysical Chemistry*, Freeman, San Francisco (1980).
Cooney, D. O., and C. L. Jim, "Solvent Extraction of Phenol from Aqueous Solution in a Hollow-Fiber Device," Anaheim AIChE Meet. (1984).
Cussler, E. L., *Diffusion*. Cambridge, London (1984).
Dahuron, L., "Designing Liquid-Liquid Extractions in Hollow-Fiber Modules," Ph.D. Thesis, Univ. Minnesota, Minneapolis (1987).
D'Elia, N. A., "Liquid-Liquid Extraction in Hollow-Fiber Modules," M.S. Thesis, Univ. Minnesota, Minneapolis (1985).
———, L. Dahuron, and E. L. Cussler, "Liquid-Liquid Extractions with Microporous Hollow Fibers," *J. Memb. Sci.*, **29**, 309 (1986).
Göklen, K. E., and T. A. Hatton, "Liquid-Liquid Extractions of Low Molecular Weight Proteins by Selective Solubilization in Reversed Micelles," *Sep. Sci. Tech.*, **22**, 831 (1987).
Hiss, T. G., and E. L. Cussler, "Diffusion in High Viscosity Liquids," *AIChE J.*, **19**, 698 (1973).
Kiani, A., R. R. Bhave, and K. K. Sirkar "Solvent Extraction with Immobilized Interfaces in Microporous Membrane, *J. Memb. Sci.*, **20**, 125 (1984).
Kim, B. M., "Membrane-based Solvent Extraction for Selective Removal and Recovery of Metals," *J Memb. Sci.*, **21**, 5 (1984b).
Komiyama, J., and R. M. Fuoss, "Conductance in Water-Polyvinyl Alcohol Mixtures," *Proc. Nat. Acad. Sci.*, **69**, 829 (1972).
Kreith, F., and W. Z. Black, *Basic Heat Transfer*, Harper and Row, Cambridge (1980).
Kula, K., H. Kroner, and H. Hustedt, "Purification of Enzymes by Liquid-Liquid Extraction," *Adv. Biochem. Eng.*, **24**, 73 (1982).
Lévêque, M. A., "Les Lois de la Transmission de Chaleur par Convection," *Ann. Mines ou Recuell de Memories sur L'Explotasion des Mines* (d12e series) **13**, 201 (1928).
Matson, S. L., J. Lopez, and J. A. Quinn, "Separation of Gases with Synthetic Membranes," *Chem. Eng. Sci.*, **38**, 503 (1983).
Prasad, R., A. Kiani, R. R. Bhave, and K. K. Sirkar, "Further Studies on Solvent Extraction with Immobilized Interfaces in a Microporous Hydrophobic Membrane" *J. Memb. Sci.*, **26**, 79–97 (1986).
Prasad, R., and K. K. Sirkar, "Dispersion-Free Solvent Extraction with Microporous Hollow-Fiber Modules," *AIChE J.* **33**, 1057 (1987).
Sieder, E. N., and G. E. Tate, "Heat Transfer and Pressure Drop of Liquids in Tubes," *Ind. Eng. Chem.*, **28**, 1429 (1936).
Snell, F. D., and Hitton, C. L., eds., *Encylcopedia of Industrial Chemical Analysis*, Interscience, New York (1966).
Treybal, R. E., *Mass Transfer Operations*, 3rd ed., McGraw-Hill, New York (1980).
Yang, M. C., and E. L. Cussler, "Designing Hollow-Fiber Contactors," *AIChE J.*, **32** 1910 (1986).
Zhang, Qi, and E. L. Cussler, "Microporous Hollow Fibers for Gas Absorption," *J. Memb. Sci.*, **23**, 321 (1985a).
———, "Hollow-Fiber Gas Membranes," *J. Memb. Sci.*, **31**, 1548 (1985b).
Zubay, G., *Biochemistry*, Addison-Wesley, Reading, MA (1983).

Manuscript received Apr. 29, 1987, and revision received July 9, 1987.